

Ising string beyond the Nambu-Goto action

Alberto Baffigo and Michele Caselle 

Department of Physics, University of Turin and INFN, Turin Via Pietro Giuria 1, I-10125 Turin, Italy



(Received 5 January 2024; accepted 1 February 2024; published 28 February 2024)

A major result of the effective string theory (EST) description of confinement is the so-called “low-energy universality”, which states that the first few terms of the large distance expansion of any EST are universal and coincide with those of the Nambu-Goto action. Going beyond this approximation is one of the most interesting open problems in the EST. In the higher-order terms beyond Nambu-Goto several important pieces of physical information are encoded, which could improve our understanding of the physical mechanisms behind confinement and of the physical degrees of freedoms which originate the EST. In this paper we evaluate numerically the first two of these corrections in the case of the three-dimensional gauge Ising model. The first of them turns out to be negative; $\gamma_3 = -0.00048(4)$, similar (but not equal) to the one recently measured in the $SU(2)$ Yang-Mills theory in three dimensions and compatible with the bootstrap bound $\gamma_3 \geq -\frac{1}{768}$.

DOI: [10.1103/PhysRevD.109.034520](https://doi.org/10.1103/PhysRevD.109.034520)

I. INTRODUCTION

One of the most promising approaches to understand and model the nonperturbative behavior of confining Yang-Mills theories is the effective string theory (EST) description in which the confining flux tube joining together a quark-antiquark pair is modeled as a thin vibrating string [1–5].

Recently, there has been a lot of progress in this context. In particular it has been realized that the EST enjoys the so-called “low-energy universality” [6–13] which states that, due to the peculiar features of the string action and to the symmetry constraints imposed by the Poincaré invariance in the target space, the first few terms of its large distance expansion are fixed and are thus universal. This implies that the EST is much more predictive than typical effective models and in fact its predictions have been successfully compared in the past few years with lot of results on the interquark potential from Monte Carlo simulations in lattice gauge theories (LGTs) (for recent reviews see for instance [13–15]).

At the same time it was recently realized that the simplest, Lorentz invariant, EST which is the well-known Nambu-Goto model [1,2] is an exactly integrable, irrelevant, perturbation of the bidimensional free Gaussian model [10], driven by the $T\bar{T}$ operator of the $D - 2$ free

bosons¹ [16] which represent the transverse degree of freedom of the string. This observation stimulated lot of interesting results even beyond the original application to Yang-Mills theories [17–24]. In particular they are at the basis of a S-matrix bootstrap approach which can be used to constrain the EST action even beyond the Nambu-Goto approximation [25,26].

Indeed, it is by now clear that the Nambu-Goto action should be considered only as a first-order approximation of the actual EST describing the nonperturbative behavior of the Yang-Mills theories. Going beyond this approximation is one of the most interesting open problems in this context. In the higher-order terms beyond Nambu-Goto several important pieces of physical information are encoded. Their study could be of great importance to understand the physical mechanisms behind confinement or the physical degrees of freedoms which originate the EST.

In particular, it is only by looking at these higher-order terms that one may hope to find signatures, in the confining string, of the gauge group of the underlying LGT. For this reason there is an increasing interest in exploring these corrections in different LGTs [27]. In this respect the three-dimensional gauge Ising model that we shall study in this paper is a perfect laboratory to address this issue because, thanks to the duality transformation with the 3D Ising model, one can use innovative, powerful, algorithms to estimate these corrections. Moreover, its gauge symmetry is very different from standard $SU(N)$ gauge groups and

Published by the American Physical Society under the terms of the Creative Commons Attribution 4.0 International license. Further distribution of this work must maintain attribution to the author(s) and the published article's title, journal citation, and DOI. Funded by SCOAP³.

¹We shall denote in the following with D the number of spacetime dimensions of the target LGT and with $d \equiv D - 1$ the number of spacelike directions.

allows to test, for instance, which is the effect of the discrete vs continuous gauge symmetries on the confining string. A final important reason is that the scaling function of the string tension, which will play a central role in the following, is known (thanks again to duality) with very high precision.

Due to the low-energy universality these corrections appear at a very high order in the large distance expansion and their evaluation is a delicate task. One must reach very precise estimates of the ground state energy of the string for a wide range of distances and, possibly, for a few different values of β to test the correct scaling behavior. For these reasons we decided to evaluate them with two different approaches, using different algorithms (hierarchical Metropolis in one case and Swendsen-Wang in the other) choosing different observables (the ground-state energy of the string in one case and its width in the other) and looking for an overall agreement of the final results between the two methods.

We were able to detect the first two corrections beyond Nambu-Goto which are described, as we shall see below, by the two parameters γ_3 and γ_5 [25]. The value of $\gamma_3 = -0.00048(4)$ agrees with the S-matrix bound found in [25] and is similar, but slightly more negative than the value $\gamma_3|_{SU(2)} = -0.00037(6)$ found in [27] for the $SU(2)$ LGT in $(2+1)$ dimensions. The second correction is very small $\gamma_5 = 3.0(4) \times 10^{-7}$ but not compatible with zero and its inclusion in the fit turned out to be mandatory to reach reasonable values of the reduced χ^2 . These values represent the first step toward a systematic study of γ_3 in LGTs.

This paper is organized as follows. In the Sec. II we shall define the problem and set the notations, then in Sec. III we shall recall a few basic results of the effective string theory of confinement. In Sec. IV we shall present the 3D gauge Ising model and discuss its properties. Then, in Secs. V and VI, we shall discuss the two approaches that we used to evaluate γ_3 and γ_5 and present the main steps of the data analysis. Finally the last section is devoted to a summary of the results and a few concluding remarks.

II. GENERAL SETTING AND NOTATIONS

In the following we shall be mainly interested in finite temperature LGTs, which can be realized by imposing periodic boundary conditions in the time direction for the bosonic field (and antiperiodic for fermionic ones). In a finite temperature setting the compactified “time” direction does not have any longer the meaning of time (recall that we are describing a system at equilibrium in the canonical ensemble) but its size N_t is instead a measure of the inverse temperature of the system. Thus, a lattice of size $N_s a$ in the spatial directions and $N_t a$ in the timelike direction represents the regularized version of a system of finite volume $V = (N_s a)^d$ at a finite temperature $T = 1/(N_t a)$. In the following we shall set the lattice spacing to $a = 1$, and systematically neglect it.

In a finite temperature setting one can define a new class of topologically nontrivial observables which are gauge invariant thanks to the periodic boundary conditions in the time direction; the Polyakov loops. If we define the link dynamical variables of the gauge model as $U_\mu(\vec{x}, z)$ [where μ denotes the direction of the link and (\vec{x}, z) its coordinates in the lattice], we may define the Polyakov loop $P(\vec{x})$ as follows:

$$P(\vec{x}) = \text{Tr} \prod_{z=1}^{N_t} U_t(\vec{x}, z). \quad (1)$$

In a pure LGT the Polyakov loop acquires a nonzero expectation value in the deconfined phase and is thus an order parameter of the finite temperature deconfinement transition.

The value $\beta_c(N_t)$ of this deconfinement transition in a lattice of size $N_t = 1/T$ can be used to define a new physical observable T_c which is obtained by inverting $\beta_c(N_t)$. We obtain in this way, for each value of β , the lattice size in the time direction [which we shall call in the following $N_{t,c}(\beta)$] at which the model undergoes the deconfinement transition and from this the critical temperature $T_c(\beta) \equiv 1/N_{t,c}(\beta)$ as a function of β . We shall use this quantity to set the scale of our simulations.

In the following we shall be mainly interested in correlators of Polyakov loops:

$$G(R, N_t) \equiv \langle P(x) P^\dagger(x+R) \rangle_{N_t}, \quad (2)$$

where R is the distance between the two Polyakov loops and the subscript N_t in the expectation value reminds that the correlator was evaluated on a lattice at temperature $T = 1/N_t$. $G(R, N_t)$ can be used to define a finite temperature version of the interquark potential:

$$V(R, T) = -\frac{1}{N_t} \log \langle P(x) P^\dagger(x+R) \rangle_{N_t}. \quad (3)$$

In the confining phase we expect, for large values of R , a linearly rising behavior for $V(R, N_t)$, which implies the following behavior for the correlator:

$$\langle P(x) P^\dagger(x+R) \rangle_{N_t} \sim e^{-E_0(T)N_t R}. \quad (4)$$

From Eq. (4) we may extract the ground state energy $E_0(T)$ of the confining flux tube joining the quark-antiquark pair. $E_0(T)$ depends on the temperature of the model and vanishes at the deconfinement transition. The finite temperature behavior of $E_0(T)$ will play a major role in the rest of the paper. It is interesting to notice that the observable (2) has the topology of a cylinder whose circumference is fixed by the (inverse) temperature N_t and the length by the interquark distance R .

III. EFFECTIVE STRING THEORY

A. The Nambu-Goto action

The behavior of the flux tube in a confining LGT is well-described by the effective string theory which models the flux tube as a thin vibrating string and allows to evaluate the contribution to the Polyakov-loop correlator of the quantum fluctuations of this flux tube.

The simplest possible EST fulfilling the constraints imposed by the Lorentz invariance in the target space is the Nambu-Goto action [1,2] defined as follows:

$$S_{\text{NG}} = \sigma_0 \int_{\Sigma} d^2\xi \sqrt{g}, \quad (5)$$

where $g \equiv \det g_{\alpha\beta}$ and

$$g_{\alpha\beta} = \partial_{\alpha} X_{\mu} \partial_{\beta} X^{\mu} \quad (6)$$

is the metric induced on the reference world-sheet surface Σ by the mapping $X_{\mu}(\xi)$ of the world sheet in the target space, and $\xi \equiv (\xi^0, \xi^1)$ denote the world sheet coordinates. This term has a simple geometric interpretation; it measures the area of the surface spanned by the string in the target space and has only one free parameter² which is the string tension σ_0 .

In order to perform calculations with the Nambu-Goto action one has first to fix its reparametrization invariance. The standard choice is the so-called ‘‘physical gauge’’. In this gauge the two world sheet coordinates are identified with the longitudinal degrees of freedom of the string, $\xi^0 = X^0$, $\xi^1 = X^1$, so that the string action can be expressed as a function only of the $(D-2)$ degrees of freedom corresponding to the transverse displacements, X^i , with $i = 2, \dots, (D-1)$ which are assumed to be single-valued functions of the world sheet coordinates. We shall comment below on the problems of this gauge fixing choice.

With this gauge choice the determinant of the metric can be written as

$$g = 1 + \partial_0 X_i \partial_0 X^i + \partial_1 X_i \partial_1 X^i + \partial_0 X_i \partial_0 X^i \partial_1 X_j \partial_1 X^j - (\partial_0 X_i \partial_1 X^i)^2 \quad (7)$$

and the Nambu-Goto action can then be written as a low-energy expansion in the number of derivatives of the transverse degrees of freedom of the string which, by a suitable redefinition of the fields, can be rephrased as a large distance expansion,

²We shall denote in the following the string tension with the index 0 to avoid confusion with the spin variables of the Ising model.

$$S = S_{\text{cl}} + \frac{\sigma_0}{2} \int d^2\xi [\partial_{\alpha} X_i \cdot \partial^{\alpha} X^i + \dots]. \quad (8)$$

The first term of this expansion is exactly the gaussian action, i.e. a two-dimensional conformal field theory (CFT) of $D-2$ free bosons which represent the transverse degrees of freedom of the string, and the remaining terms combine themselves so as to give an exactly integrable, irrelevant perturbation of this CFT [10], driven by the $T\bar{T}$ operator of the $D-2$ free bosons [16].

Thanks to this exact integrability, the partition function of the model can be written explicitly [7,28]. For the Polyakov-loop correlator in which we are interested here,³ the expression in D space-time dimensions is, using the notations of [7,28],

$$\langle P(x) P^{\dagger}(x+R) \rangle_{N_t} = \sigma_0^{\frac{4-D}{2}} \frac{N_t}{\pi} \sum_{n=0}^{\infty} w_n \left(\frac{E_n}{2R} \right)^{\frac{1}{2}(D-3)} \times K_{\frac{1}{2}(D-3)}(E_n R), \quad (9)$$

where $K_{\frac{1}{2}(D-3)}$ is the modified Bessel function of order $\frac{D-3}{2}$, R denotes, as above, the distance between the two Polyakov loops, N_t the size of the lattice in the compactified direction, w_n is the multiplicity of the closed string states which propagate from one Polyakov loop to the other, and E_n their energies:

$$E_n = \sigma_0 N_t \sqrt{1 + \frac{8\pi}{\sigma_0 N_t^2} \left[-\frac{1}{24}(D-2) + n \right]}. \quad (10)$$

At large distances, the correlator is dominated by the lowest state

$$E_0 = \sigma_0 N_t \sqrt{1 - \frac{\pi(D-2)}{3\sigma_0 N_t^2}}, \quad (11)$$

whose multiplicity is $w_0 = 1$ and the Polyakov-loop correlator, neglecting irrelevant constants, reduces to

$$\langle P(x) P^{\dagger}(x+R) \rangle_{N_t} \sim \sigma_0^{\frac{4-D}{2}} N_t \left(\frac{E_0}{R} \right)^{\frac{1}{2}(D-3)} K_{\frac{1}{2}(D-3)}(E_0 R) \quad (12)$$

which, in the $D=3$ case in which we are interested simplifies to

$$\langle P(x) P^{\dagger}(x+R) \rangle_{N_t} \sim N_t \sqrt{\sigma_0} K_0(E_0 R) \quad (13)$$

with

³Similar expressions can be obtained also for the other relevant geometries: the Wilson loop [29] and the interface [30].

$$E_0 = \sigma_0 N_t \sqrt{1 - \frac{\pi}{3\sigma_0 N_t^2}}. \quad (14)$$

Thanks to the exponential term in the asymptotic expansion of the Bessel function,

$$K_0(z) = \sqrt{\frac{\pi}{2z}} e^{-z} \left[1 - \frac{1}{8z} + \frac{9}{128z^2} + \mathcal{O}(z^{-3}) \right] \quad (15)$$

we find at large distance, as expected, a linearly rising behavior of the interquark potential controlled by the ground state energy E_0 . On top of this we have a set of subleading corrections, encoded in the asymptotic expansion of K_0 , which represent a specific, unique, signature of the Nambu-Goto action and must be taken into account when fitting the results of Monte Carlo simulations.

An important side consequence of this result is that we can extract from the tachyonic singularity of E_0 an estimate for the critical temperature $T_{c,\text{NG}}$ measured in units of the square root of the string tension $\sqrt{\sigma_0}$ [31,32] which is, for generic values of D ,

$$\frac{T_{c,\text{NG}}}{\sqrt{\sigma_0}} = \sqrt{\frac{3}{\pi(D-2)}} \quad (16)$$

and corresponds to the value of the ratio $\frac{T_{c,\text{NG}}}{\sqrt{\sigma_0}}$ for which the ground-state energy E_0 vanishes. Using this result we can rewrite the ground state energy as

$$E_0(T)|_{\text{NG}} = \frac{\sigma_0}{T} \sqrt{1 - \frac{T^2}{T_{c,\text{NG}}^2}}, \quad (17)$$

where we use the notation $|_{\text{NG}}$ to stress the fact that this is only the Nambu-Goto estimate for the ground state energy of the string, which we may expect to be modified by other terms in the EST action.

The estimate quoted above for the critical temperature turns out to be in remarkable (but not exact!) agreement with the results obtained from Monte Carlo simulations, both for non-Abelian LGTs and for the three-dimensional gauge Ising model. However, the remaining small deviations of $T_{c,\text{NG}}$ from the Monte Carlo results, together with the fact that the Nambu-Goto EST predicts [as can be seen looking at Eq. (17)] a deconfinement transition of the second order, with a mean field value for the critical index (which is in disagreement with the Monte Carlo results for all known LGTs) suggest that the Nambu-Goto action cannot be the end of the story and that some correcting terms beyond Nambu-Goto should be present in the EST.

B. Beyond Nambu-Goto

It is by now clear that in the actual EST of the confining string the Nambu-Goto action is only the first term of an

infinite series of contributions. Indeed, there are several reasons why the Nambu-Goto action is unsatisfactory and must be completed with some higher-order correction. Besides the above mentioned disagreement at the deconfinement transition, a major problem of the Nambu-Goto action is that it is, so to speak, too universal. It predicts the same behavior for all LGTs, with no dependence on the gauge group. Moreover, it is well-known that the physical gauge fixing discussed above is anomalous and it is widely expected that this anomaly could be cured by higher-order terms in the EST action.

The requirement of Poincarè invariance in the target space strongly constrains the terms which can be included in the EST beyond Nambu Goto [6–13]. In $D = 3$ the first few allowed terms can be written as follows:

$$S_{\text{EST}} = \int_{\Sigma} d^2\xi \sqrt{g} [\sigma_0 + \gamma_1 \mathcal{R} + \gamma_2 K^2 + \gamma_3 K^4 \dots], \quad (18)$$

where the γ_i are new coupling constants, \mathcal{R} denotes the Ricci scalar constructed from the induced metric, and K is the extrinsic curvature, defined as $K = \Delta(g)X$, with

$$\Delta(g) = \frac{1}{\sqrt{(g)}} \partial_a [\sqrt{(g)} g^{ab} \partial_b] \quad (19)$$

the Laplacian in the space with metric $g_{\alpha\beta}$. In principle the new coupling constants γ_i , should be fixed, as we do for σ_0 , by comparing with experiments (or more likely, with computer simulations).

However this process is simplified by the observation that K^2 vanishes on shell and that the term proportional to \mathcal{R} is a topological invariant in two dimensions. Since in the long-string limit in which we are interested one does not expect topology-changing fluctuations, both these terms can be neglected and the first nontrivial contribution appears only at higher orders [13]. This result is known as “low-energy universality” [10] and strongly constrains the form of the EST. It implies that the first correction beyond the Nambu-Goto action can only appear at the order $1/R^7$ (or $1/N_t^7$ in the finite temperature setting in which we are interested in this paper). This explains why the Nambu-Goto model has been so successful over these last forty years to describe the infrared behavior of confining gauge theories despite its simplicity and why the deconfinement temperature predicted by Nambu-Goto is so close to the one obtained in Monte Carlo simulations. At the same time this explains why identifying these corrections is so difficult and only in the last few years it was possible to unambiguously detect them in Monte Carlo simulations [19,27,33–35].

The first nonvanishing term $\gamma_3 K^4$ is only the first of an infinite sequence of terms, obtained combining higher-order curvature invariants. It turns out that the best way to organize these terms is to study the $2 \rightarrow 2$ scattering amplitude of the string excitations [10]. It can be shown

that in $D = 3$ this S-matrix $S = e^{2i\delta}$ can be written in a particularly simple and elegant form:

$$2\delta(s) = \frac{s}{4} + \gamma_3 s^3 + \gamma_5 s^5 + \gamma_7 s^7 + i\gamma_8 s^8 + O(s^9), \quad (20)$$

where the first term $s/4$ leads to the energy spectrum of the Nambu-Goto action, the fact that the term proportional to s^2 is missing is the way in which the low energy universality is realized in this S-matrix approach and the next nontrivial term is exactly the S-matrix description of the K^4 correction mentioned above.

By using the analyticity properties of this S-matrix and requiring the UV completion of the underlying theory it is possible to obtain a set of important results on the ground-state energy of the string [10,25]:

- (i) γ_8 is not a new independent parameter but it is proportional to γ_3^2 ;
- (ii) Both the $1/N_t^7$ and the $1/N_t^9$ terms are controlled only by γ_3 and the next independent parameter γ_5 only appears at the order $1/N_t^{11}$;
- (iii) It is possible to set bounds on these parameters. In particular, defining

$$\tilde{\gamma}_n = \gamma_n + (-1)^{(n+1)/2} \frac{1}{n2^{3n-1}}$$

one finds [25]

$$\begin{aligned} \tilde{\gamma}_3 &\geq 0 \\ \tilde{\gamma}_5 &\geq 4\tilde{\gamma}_3^2 - \frac{1}{64}\tilde{\gamma}_3 \\ \tilde{\gamma}_7 &\geq \frac{\tilde{\gamma}_5^2}{\tilde{\gamma}_3} + \frac{1}{4096}\tilde{\gamma}_3 + \frac{1}{64}\tilde{\gamma}_5 - \frac{1}{16}\tilde{\gamma}_3^2 \end{aligned} \quad (21)$$

which implies in particular

$$\gamma_3 \geq -\frac{1}{768}. \quad (22)$$

From the S-matrix, by using the so-called thermodynamic Bethe ansatz one can obtain [25] the following expression for the nonuniversal corrections up to the order $1/N_t^{11}$:

$$\begin{aligned} E_0(N_t) = \sigma_0 N_t \sqrt{1 - \frac{\pi}{3\sigma_0 N_t^2}} - \frac{32\pi^6 \gamma_3}{225\sigma_0^3 N_t^7} \\ - \frac{64\pi^7 \gamma_3}{675\sigma_0^4 N_t^9} - \frac{2\pi^8 \gamma_3}{45} + \frac{32768\pi^{10} \gamma_5}{3969} \\ - \frac{1}{\sigma_0^5 N_t^{11}}. \end{aligned} \quad (23)$$

This is the expression which we shall compare with the results of our simulations.

C. The boundary corrections problem and how to deal with it

It is clear from the previous section that measuring the γ_i coefficients on the lattice is a highly nontrivial task. In particular it is essentially impossible in the standard ‘‘zero temperature’’ scenario, in which the contribution of the effective string to the interquark potential manifests itself as an expansion in powers of $1/R$ and the corrections in which we are interested, which appear in this expansion at the order $1/R^7$, are shadowed by the boundary corrections which are proportional to $1/R^4$ [11,36–39].

There are in principle two ways to avoid this problem:

- (i) The first is to study observables without boundaries. This can be done for Abelian gauge models using duality and looking at the finite size effects of the interface free energy (choosing interfaces with periodic boundary conditions) [40,41]. In the case of the Ising model this approach was recently discussed in [42] where it was shown that corrections beyond Nambu-Goto certainly exist in the gauge Ising model and are rather large. However, it turned out to be difficult to quantify these corrections, most probably due to the interactions between nearby interfaces.⁴

- (ii) The second is to study the model in the finite temperature regime (just below the deconfinement transition) in the limit of very large separation of the two Polyakov loops ($R \gg N_t$). It can be shown that in this regime the boundary corrections become subleading and can be neglected [15,43]. Moreover, this is exactly the limit discussed in the previous section, in which the results obtained with the S-matrix approach and TBA hold. Thus, by choosing this geometry in our simulations we shall be able to make immediate contact with Eq. (23), with no interference from the boundary terms and extract from the data reliable estimates for the γ_i coefficients. This was the approach recently used to study these corrections in the $SU(2)$ gauge model in three dimensions in [27].

Once the geometry of the observables in which we are interested is fixed, the remaining task is to obtain estimates for these observables precise enough to detect and quantify the tiny corrections in which we are interested. In this geometry this requires studying the system at large interquark distances and standard algorithms are affected by an

⁴The way in which these interfaces are generated in the (dual) gauge Ising model is by fixing antiperiodic boundary conditions in the transverse direction. This procedure generates an odd number of interfaces. This ensemble is usually studied assuming that they are far apart and do not interact, but when looking at very asymmetric geometries (which are needed in order to detect higher-order corrections) the width of these interfaces grows linearly and neglecting interactions is most likely a too strong approximation.

exponentially decreasing signal to noise ratio in this limit. The main advantage of studying Abelian models is that, thanks to duality, it is possible to avoid this limitation and to study (using for instance nonlocal cluster algorithms as in [44] or the so-called “snake algorithm” [45]) Polyakov loops correlators at any interquark distance R with the same signal to noise ratio. This is the main reason behind the choice of the Ising model as a laboratory to study the EST.

There is indeed a long track record of applications of this kind of methods to the 3D gauge Ising model to study subtle features of EST. In particular, in [44,46–48] which may be considered as precursors of the present work, the $1/R^3$ correction to the interquark potential was precisely measured for the first time and shown to be exactly the one predicted by the Nambu-Goto action (in agreement with the low-energy universality). Later the same approach was adopted for the 3D $U(1)$ model in [49] and allowed to unambiguously detect corrections to the Nambu-Goto actions as the continuum limit was approached.

In Sec. V we discuss the result of a study performed with the same snake algorithm used in [46,47]. This algorithm allowed us to obtain a first estimate of γ_3 which however turned out to be affected by a rather large statistical uncertainty. In order to improve this uncertainty and to test the robustness of the result we decided to evaluate the same quantity with a completely different method, which was proposed a few years ago in [50] and that we describe in detail in Sec. VI.

This second estimate agrees within the errors with the previous one, is more precise and allows to quantify with rather good precision even the next to leading correction γ_5 . The agreement between the two estimates strongly supports the reliability of our analysis.

In the following sections we shall first describe the main features of the 3D gauge Ising model and then discuss the two approaches that we used to evaluate the γ_i coefficients.

IV. THE 3D GAUGE ISING MODEL

The three-dimensional gauge Ising model (also known as \mathbb{Z}_2 gauge model) was proposed over fifty years ago by Wegner [51] as a tool for understanding the properties of lattice models with gauge symmetries. This model exhibits a local \mathbb{Z}_2 symmetry, which is realized by the choice of $\sigma_l \in \{1, -1\}$ as the dynamical \mathbb{Z}_2 link variables. The plaquette action, derived from the familiar Wilson action, is tailored specifically for the case of \mathbb{Z}_2 link variables and can be defined as follows:

$$Z_{\text{gauge}}(\beta) = \sum_{\{\sigma_l = \pm 1\}} \exp(-\beta S_{\mathbb{Z}_2}). \quad (24)$$

The action $S_{\mathbb{Z}_2}$ is a sum over all the plaquettes of a cubic lattice,

$$S_{\mathbb{Z}_2} = - \sum_{\square} \sigma_{\square}, \quad \sigma_{\square} = \sigma_{l_1} \sigma_{l_2} \sigma_{l_3} \sigma_{l_4}. \quad (25)$$

Despite its apparent simplicity the 3D Gauge Ising Model shares with more complex LGTs several important properties. It is characterized by a confining string with a nontrivial spectrum of string excitations [52,53] and has a glueball spectrum very similar to the one of more complex 3D LGTs [54]. For these reasons it is a perfect laboratory to test, with high precision, nontrivial properties of the confining strings in LGTs.

This model is known to have a bulk (i.e. at zero temperature) deconfinement transition at $\beta_c = 0.76141330(6)$ (this value is obtained via duality from the critical temperature of the 3D Ising model quoted in [55], see below). For values of the coupling $\beta < \beta_c$ the model is in the confining phase, while for $\beta > \beta_c$ it is deconfined. The transition at $\beta = \beta_c$ is of second order and, due to the duality relation (see below), it belongs to the same universality class of the standard magnetization transition of the 3D Ising model. This model also possesses an (infinite-order) “roughening transition” at $\beta_r = 0.47542(1)$ [56] (in the confined phase), which separates the strong coupling regime (for $\beta < \beta_r$) from the so-called “rough phase” (for $\beta_r < \beta < \beta_c$).

In the following we shall be interested in the behavior of the model in the confining phase, in the scaling region near the critical point. In particular we shall study the model at three different values of the coupling constant β (see Table I), for which the (finite) deconfinement temperature is known with high precision [57] so as to be able to precisely set the scale for the distances between Polyakov loops and for the lattice size in the time direction (i.e. the inverse of the finite temperature of the model). These values are all located in the rough phase and close enough to β_c so as to be within the scaling region.

The major reason of interest of this model is that it is related to the ordinary three-dimensional Ising spin model by an exact duality mapping *à la* Kramers and Wannier (see Ref. [58] for a general review on duality transformations):

$$Z_{\text{gauge}}(\beta) \propto Z_{\text{spin}}(\tilde{\beta}), \quad \text{with} \quad \tilde{\beta} = -\frac{1}{2} \log [\tanh(\beta)], \quad (26)$$

TABLE I. Some information on the three values of β , listed in the first column, which we chose for the simulations. In the second column we report the corresponding values of $\tilde{\beta}$ for the (dual) 3D Ising model. In the last three columns we report respectively the (inverse of) the deconfinement temperature, the string tension (taken from Ref. [41]) and the value of α [see below for the definition of $\alpha(\beta)$ and its evaluation from the scaling function of the model].

β	$\tilde{\beta}$	$N_{t,c}$	σ	α
0.751800	0.226104	8	0.0105255(11)	0.4576(4)
0.756427	0.223951	12	0.0046384(26)	0.3887(3)
0.758266	0.223101	16	0.0026043(53)	0.3464(2)

where the Ising spin model is defined by the usual action,

$$Z_{\text{spin}} = \sum_{\{s_i\}} \exp\left(\tilde{\beta} \sum_{\langle i,j \rangle} s_i s_j\right), \quad (27)$$

where, as usual, the $s_i \in \{1, -1\}$ are \mathbb{Z}_2 spin variables, the i and j indices denote the sites of the dual lattice, the notation $\sum_{\langle i,j \rangle}$ means that spin variables interact with their nearest-neighbors only and $\sum_{\{s_i\}}$ denotes the sum over spin configurations.

The critical temperature of the model is known with remarkable precision $\beta_c = 0.22165462(2)$ [55], moreover thanks to the recent advances in the bootstrap approach [59,60] also the critical indices of the two relevant operators, the magnetization M and the energy ϵ , are known with high precision: $\Delta_M = 0.5181489(10)$ and $\Delta_\epsilon = 1.412625(10)$ respectively [59,60]. From Δ_ϵ we can extract the critical index $\nu = \frac{1}{3-\Delta_\epsilon} = 0.6299708\dots$. Thanks to duality this is the same critical index which drives the critical behavior of the string tension in the 3D gauge Ising model. More precisely $\sigma(\beta) \sim \sigma_c(\beta_c - \beta)^{2\nu}$. We shall further discuss the scaling behavior of the string tension in the Appendix.

The main reason of interest of this mapping is that a similar construction can be performed also in presence of external source terms for the gauge model (for instance, a pair of Polyakov loops). This can be easily realized by introducing sets of topological defects in the spin system. As a result, it is possible to show [46] that, for instance, the Polyakov-loop correlator in which we are interested is mapped into the partition function of the spin system with antiferromagnetic coupling on a well-defined set of links,

$$G(r) \equiv \langle P(x)P^\dagger(x+R) \rangle_{N_t} = \frac{Z_{\text{spin},Q\bar{Q}}(R, N_t)}{Z_{\text{spin}}} \quad (28)$$

with

$$Z_{\text{spin},Q\bar{Q}}(R, N_t) = \sum_{\{s_i\}} \exp\left(\tilde{\beta} \sum_{\langle i,j \rangle} J_{\langle i,j \rangle} s_i s_j\right), \quad (29)$$

where the value of the $J_{\langle i,j \rangle}$ coupling is $+1$ everywhere, except on a set of bonds, which pierce a surface (in the direct lattice) having the source worldlines as its boundary; for such a set of bonds, $J_{\langle i,j \rangle} = -1$.

Similar mappings can be constructed essentially for any observable of interest in the gauge model, from Wilson loops to glueball correlators.⁵

⁵For instance it can be shown in this way that the glueballs of the Ising gauge model are mapped into bound states of the fundamental scalar in the spin model [61].

Both the numerical algorithms that we shall use in the following exploit this duality of the model, simulating the Ising spin system, and measuring (the first algorithm) ratios of partition functions associated with different stacks of defects (which we shall use to express the expectation values of Polyakov loops pairs in the original gauge model) or expectation values of spins in presence of the defect surface (the second algorithm).

A particularly useful advantage of numerical simulations in the dual setting is the fact that this method overcomes the problem of exponential signal-to-noise ratio decay, which is usually found when studying the interquark potential $V(r)$ at larger and larger distances.

Another important feature is that, thanks to duality, the values of the Polyakov-loop correlators that we obtain in this way are not affected by corrections due to the periodic boundary conditions in the spacelike directions. This greatly simplifies the study of these correlators (no additional terms must be included in the fits to keep into account these corrections) and allow to study the system for (relatively) small lattice size in the spacelike directions.

We performed simulations for the three values of β quoted in Table I; $\beta = 0.751800, 0.756427, 0.758266$ which were chosen because for these values the deconfinement temperature is known with very high precision and coincides with $1/T_c = L_c = 8, 12, 16$, respectively [57].

V. ANALYSIS WITH THE SNAKE ALGORITHM

The first method that we used to estimate γ_3 is the Ising implementation of the snake algorithm [45] discussed in detail in [46]. The main feature of the algorithm is the hierarchical organization of the updates. In our particular implementation we chose five sublattice levels with size $\{6, 13, 17, 21, 24\}$ lattice spacings respectively.

We studied the first two values of β reported in Table I corresponding to a deconfinement temperature of $N_{t,c} = 8$ and $N_{t,c} = 12$, respectively. Details on the simulations are reported in Table II. For each β we studied seven values of N_t just above the critical value $N_{t,c}$ (i.e. just below the deconfinement temperature). Then for each value of N_t we simulated eight different values of R as reported in the table. The value of the lattice size in the space direction was chosen to be ten times the value of $N_{t,c}$ to avoid finite size effects (which in any case are strongly suppressed thanks to the duality transformation). The values of R were chosen so as to make higher-order energy levels in Eq. (9) negligible within the errors. Thus we could fit the R dependence of our Polyakov loop correlators using Eq. (13). From the snake algorithm we directly obtain the ratio of two nearby correlators $F(R, N_t) = G(R+1, N_t)/G(R, N_t)$ which we thus fitted with the following expression:

TABLE II. Some information on the simulations.

β	$N_{t,c}$	N_t	R	N_s
0.751800	8	9, 10, 11, 12, 14, 16, 18	8, 12, 16, 20, 24, 32, 40, 48	80
0.756427	12	13, 14, 15, 16, 18, 20, 24	18, 24, 30, 36, 48, 60, 72, 84	120

$$F(R, N_t) = \frac{K_0(E_0(N_t)(R+1))}{K_0(E_0(N_t)R)} \quad (30)$$

with $E_0(N_t)$ as the only free parameter of the fit. For all values of N_t we found good values of the reduced χ^2 . We report in Table III, as an example of the results obtained with the snake algorithm, the values obtained for the largest Polyakov loops correlators that we studied i.e. those for $\beta = 0.756427$ and $N_t = 24$. As anticipated there is no increase in the signal to noise ratio as R increases and we could estimate the ratio of the two Polyakov-loop correlators with less than 1% error for areas as large as 24×84 lattice spacings. We report in Tables IV and V the results of these fits.

These are the values that we compared with the expectation of Eq. (23). We performed two types of fit. First, we kept as free parameters only σ_0 and γ_3 . Accordingly we truncated the square root of the Nambu-Goto action to the same order $O(N_t^9)$ at which the γ_3 terms appears. Results of these fits are reported in Table VI. Second, we included also

TABLE III. Results of the snake algorithm for $\beta = 0.756427$ and $N_t = 24$.

R	$\frac{G(R+1)}{G(R)}$
18	0.8914(29)
24	0.8969(31)
30	0.9003(32)
36	0.9030(33)
48	0.9036(33)
60	0.9035(33)
72	0.9070(35)
84	0.9085(35)

TABLE IV. Results of the fit with Eq. (30) for $\beta = 0.751800$. In the last column the reduced χ^2 of the fits.

N_t	E_0	χ_r^2
9	0.0226(11)	0.90
10	0.0419(10)	0.13
11	0.0587(9)	0.33
12	0.0776(9)	0.34
14	0.1058(9)	0.16
16	0.1337(10)	0.08
18	0.1596(10)	0.05

γ_5 and, accordingly, truncated the square root to the order $O(N_t^{11})$. The results of these fits are reported in Table VII.

A few observations on this result:

- (i) In the first type of fits the values of σ_0 that we obtain are definitely larger (more than three standard deviations) than the expected ones. Accordingly, if we try to fit the data keeping σ_0 to the expected value we also found very large values of χ^2 . Moreover, the fact that the reduced χ^2 is larger than 1 suggests that the inclusion of the next-order term in the fits could lead to non-negligible corrections and in fact the values of γ_5 in the fits truncated at $O(N_t^{11})$ are different from zero within the errors. We also tried to fit the data truncating the expansion at the order $O(N_t^7)$ and keeping only the first correction proportional to γ_3 , but we found values of σ_0 even further away from the expected values.

TABLE V. Results of the fit with Eq. (30) for $\beta = 0.756427$. In the last column the reduced χ^2 of the fits.

N_t	E_0	χ_r^2
13	0.0099(10)	0.55
14	0.0200(10)	0.44
15	0.0263(10)	0.26
16	0.0370(11)	0.31
18	0.0494(10)	0.29
20	0.0641(12)	0.21
24	0.0906(12)	0.14

TABLE VI. Results of the fits of $E_0(N_t)$ according to Eq. (23) truncated at the order $O(N_t^9)$.

β	σ_0	γ_3	χ_r^2
0.751800	0.010671(30)	-0.000357(13)	1.81
0.756427	0.004771(27)	-0.000329(13)	1.62

TABLE VII. Results of the fits of $E_0(N_t)$ according to Eq. (23) truncated at the order $O(N_t^{11})$.

β	σ_0	γ_3	γ_5	χ_r^2
0.751800	0.010629(35)	-0.00061(11)	0.00000042(11)	1.00
0.756427	0.004740(34)	-0.00051(13)	0.00000032(12)	1.53

- (ii) Including the $O(N_t^{11})$ term in the fit the values of σ_0 that we obtain move toward the expected values and for both values of β are within two standard deviations from the values reported in Table I.⁶
- (iii) Accordingly, in all these fits, if we force σ to the known values we always find unacceptably high values of the χ^2 which were associated to large deviations in the best-fit values of γ_3 and γ_5 .
- (iv) The values of γ_3 and γ_5 that we find for the two values of β are compatible with each other within the errors.

Looking at the results we see that the estimates of γ_3 and γ_5 are affected by rather large errors and are strongly influenced by the value of σ . This is due to the fact that the fit is dominated by the Nambu-Goto part of the fitting function and in particular by the σN_t term and by the Lüscher correction. It seems difficult to improve the overall precision of the result in the framework discussed in this section since the simulations (due to the peculiar structure of the snake algorithm and the need to increase the size of the lattice in the inverse temperature direction) become more and more expensive as β moves toward the continuum limit. For this reasons we decided to approach the task following a different strategy which could partially overcome these problems.

VI. USING THE MEAN FLUX DENSITY IN THE PRESENCE OF THE POLYAKOV LOOPS TO ESTIMATE THE EST GROUND-STATE ENERGY

To avoid the above problems we tried a completely different approach. Following [50] instead of looking at the interquark potential, we studied the changes induced in the flux configuration by the presence of the Polyakov loops. We shall show below that as a consequence of this choice the explicit dependence on σ_0 and on the Lüscher term vanish. This makes this observable an unique tool to explore higher-order corrections.

Another reason of interest of this approach is that it is deeply related to another important issue of the effective string description of LGTs, i.e. the study of the flux tube thickness. It can be shown that in the high-temperature regime in which we are presently interested the width of the flux tube increases linearly with the interquark distance and not logarithmically as one would naively expect [62–64]. This linear increase is related to the linear increase in the flux energy that we observe here. In both cases the slope is temperature dependent and contains information on the higher-order effective string corrections in which we are interested.

⁶This trend suggests that including even the γ_7 correction we could reach the correct values of σ_0 . We tried to include also this correction in the fits, but the value of γ_7 turned always to be compatible with zero within the errors.

The lattice operator which measures the flux through a plaquette p in presence of two Polyakov loops P, P' for a generic LGT is

$$\langle \phi(p; P, P') \rangle = \frac{\langle PP'^{\dagger} U_p \rangle}{\langle PP'^{\dagger} \rangle} - \langle U_p \rangle, \quad (31)$$

where U_p is the trace of the ordered product of the link variables along the plaquette and in our case coincides with the product σ_{\square} introduced above. This is the quantity which is typically used to study the profile of the flux tube. In our analysis we are actually interested in a much simpler observable, the mean flux density, i.e. the sum of $\phi(p; P, P')$ over all the positions and orientations of the plaquettes, normalized to the number of plaquettes of the lattice. Due to translational invariance this quantity will depend only on the distance R between the two Polyakov loops and on the inverse temperature N_t . Let us define

$$\langle \Phi(R, N_t) \rangle = \frac{1}{N_p} \sum_p \frac{\langle PP'^{\dagger} \sigma_{\square} \rangle}{\langle PP'^{\dagger} \rangle} - \langle \sigma_{\square} \rangle, \quad (32)$$

where $N_p = 3N_s^2 L$ denotes the number of plaquettes of the lattice.

It is easy to see from the definition of $G(R, N_t)$,

$$G(R, N_t) = \langle P^{\dagger}(R)P(0) \rangle_{N_t} = \frac{1}{Z} \sum_{\text{conf}} P^{\dagger}(R)P(0) e^{\beta \sum_p \sigma_{\square}} \quad (33)$$

that the mean flux density $\langle \Phi(R, N_t) \rangle$ can be written as

$$\langle \Phi(R, N_t) \rangle = \frac{1}{N_p} \frac{d}{d\beta} \log G(R, N_t). \quad (34)$$

Since β appears in the observable only through the scale $\sigma_0(\beta)$ the above equation can be rewritten as

$$\langle \Phi(R, N_t) \rangle = \frac{1}{N_p} \frac{d\sigma_0}{d\beta} \frac{d}{d\sigma_0} \log G(R, N_t). \quad (35)$$

This choice has two important consequences:

- (i) In the term proportional to R , the string tension, which was the major source of systematic uncertainty in the previous calculation, is substituted by its derivative with respect to β , which can be evaluated with high confidence thanks to the very precise knowledge we have of the scaling behavior of $\sigma_0(\beta)$.
- (ii) The first-string correction (the ‘‘Lüscher term’’) which is universal and does not depend on σ_0 disappears.

This makes the above observable a perfect tool to explore higher-order corrections of the effective string.

From Eq. (13) we have

$$N_s^2 \langle \Phi(R, N_t) \rangle = \alpha(\beta) \left(\frac{1}{2N_t \sigma_0} + \frac{K'_0(E_0 R)}{K_0(E_0 R)} \frac{R}{N_t} \frac{dE_0}{d\sigma_0} \right), \quad (36)$$

where K'_0 denotes the derivative of the K_0 Bessel function, and α is defined as

$$\alpha(\beta) = -\frac{1}{3} \frac{d\sigma_0}{d\beta}. \quad (37)$$

Using the identity $K'_0(z) = -K_1(z)$ the logarithmic derivative $K'_0(z)/K_0(z)$ can be expanded in powers of $1/z$ as follows:

$$\frac{K'(z)}{K(z)} = -\left(1 + \frac{1}{2z} - \frac{1}{z^2} + \dots\right) \quad (38)$$

which gives

$$N_s^2 \langle \Phi(R, N_t) \rangle = \alpha(\beta) (RA(N_t) + B(N_t) + C(N_t)/R), \quad (39)$$

where the three functions A , B and C are defined as follows:

$$A(N_t) = \frac{1}{N_t} \frac{dE_0}{d\sigma_0}, \quad (40)$$

$$B(N_t) = \frac{1}{2N_t E_0} \frac{dE_0}{d\sigma_0} - \frac{1}{2N_t \sigma_0}, \quad (41)$$

$$C(N_t) = -\frac{1}{8N_t E_0^2} \frac{dE_0}{d\sigma_0}. \quad (42)$$

A crucial role in the analysis is played by $\alpha(\beta)$, a precise estimate of this quantity allows to strongly constrain the results of the fits. α can be extracted from the scaling function of the model and in its determination we leverage the very precise knowledge we have of this scaling function, thanks to the bootstrap results for the critical indices of the 3D Ising model. A detailed derivation can be found in [50]. We report for completeness the main steps of the derivation in the Appendix. The values we used in the fit are listed in Table I. Once the value of α is fixed, we can use the values we obtain for $A(N_t)$ to estimate the corrections in which we are interested.⁷ By setting $x = \frac{\pi}{3\sigma_0 N_t^2}$ we see that we can express the Nambu-Goto expectation for A [see Eq. (14)] as

$$\begin{aligned} A(N_t)_{\text{NG}} &= \frac{1 - \frac{x}{2}}{\sqrt{1-x}} \\ &= 1 + \frac{x^2}{8} + \frac{x^3}{8} + \frac{15x^4}{128} + \frac{7x^5}{64} + \frac{105x^6}{1024} + \dots \end{aligned} \quad (43)$$

As anticipated the expansion starts at the order x^{-2} i.e. N_t^{-4} , this makes this observable particularly suited to evaluate higher-order corrections.

If we introduce the corrections beyond Nambu-Goto [see Eq. (23)] we find

$$\begin{aligned} A(N_t) &= A(N_t)_{\text{NG}} + \frac{864\pi^2}{25} \gamma_3 x^4 + \frac{2304\pi^2}{25} \gamma_3 x^5 \\ &\quad + \left(162\pi^2 \gamma_3 + \frac{1474560\pi^4}{49} \gamma_5\right) x^6, \end{aligned} \quad (44)$$

where the expansion of $A(N_t)_{\text{NG}}$ is truncated at the same order at which the additional terms proportional to γ_3 and γ_5 appear. This is the function which we shall use to fit the results of our simulations.

A. Numerical simulations

To estimate the function $A(N_t)$ we used again duality and mapped the Polyakov-loop correlator into the partition function of a 3D Ising spin model in which we changed the sign of the coupling of all the links dual to the surface bordered by the two Polyakov loops. This is the same method which was used in [63,65] to estimate the width of the flux tube.

We then estimated $\langle \Phi(R, N_t) \rangle$ by simply evaluating the mean value of the plaquette in presence of these frustrated links. We chose periodic boundary conditions in the original gauge Ising model. These boundary conditions are mapped by duality into a mixture of periodic and antiperiodic boundary conditions in the dual-spin model. However, we always chose N_s large enough to eliminate any contribution from the antiperiodic sectors (which are depressed by terms proportional to $e^{-\sigma_0 N_s N_t}$ or $e^{-\sigma_0 N_s^2}$).

Since, as discussed, we are interested only in the term proportional to R in $\langle \Phi(R, N_t) \rangle$, we may neglect the disconnected component $\langle U_p \rangle$ in the evaluation of $\langle \Phi(R, N_t) \rangle$. Details on the simulations can be found in Table VIII.

We performed simulations for all the three values of β reported in Table I. For each value of β and N_t we simulated several values of the distance R between the two Polyakov loops.

For each simulation we used 10^5 iterations to thermalize the lattice and then performed 10^6 measures using a Swendsen-Wang algorithm. The values of R were chosen large enough so as to make the last term in Eq. (39) negligible, thus allowing to perform a simple linear fit to extract the values of $A(N_t)$. In Table IX we report an example of the data we obtained from the simulations (to

⁷In principle we could use also $B(N_t)$ or $C(N_t)$ to extract this information, but these terms, due to their R dependence may be affected by boundary corrections, moreover their estimates from the simulations are much less precise than those of $A(N_t)$, so we neglected them in the following.

TABLE VIII. Some information on the simulations.

β	$N_{t,c}$	N_t	R	N_s
0.751800	8	9, 10, 11, 12, 16, 20, 24	16, 24, 32, 40, 48, 64	128
0.756427	12	13, 14, 15, 16, 18, 20, 24	36, 48, 60, 72, 84, 96	192
0.758266	16	17, 18, 19, 20, 21, 22, 24, 32, 48	32, 48, 64, 80, 96, 112	256

TABLE IX. Results of the algorithm for $\beta = 0.756427$ and $N_t = 24$.

R	$\langle \Phi(R, N_t) \rangle$
36	0.927589(9)
48	0.927717(9)
60	0.927872(9)
72	0.927978(9)
84	0.928115(9)
96	0.928247(9)

TABLE X. Results of the linear fits of the first two terms of Eq. (39) for $\beta = 0.751800$.

N_t	$A(N_t)$
9	1.088(23)
10	1.071(10)
11	1.053(7)
12	1.044(5)
16	1.019(2)
20	1.008(3)
24	1.003(3)

TABLE XI. Same as Table X but for $\beta = 0.756427$.

N_t	$A(N_t)$
13	1.168(26)
14	1.127(28)
15	1.096(8)
16	1.039(23)
18	1.034(33)
20	1.019(18)
24	1.034(18)

allow a comparison, we chose the same values of β and N_t reported in Table III) and in Tables X–XII the values of $A(N_t)$ extracted from these linear fits.

We then fitted these values with Eq. (44) keeping as only free parameters γ_3 and γ_5 . Results are reported in Table XIII and Fig. 1. Thanks to the high precision in the determination of α , the systematic uncertainty on γ_3 and γ_5 due to the uncertainty on α is negligible and we quote in Table XIII only the statistical errors of the fits.

TABLE XII. Same as Table X but for $\beta = 0.758266$.

N_t	$A(N_t)$
17	1.247(35)
18	1.134(9)
19	1.100(26)
20	1.114(23)
21	1.103(26)
22	1.065(12)
24	1.025(20)
32	1.005(14)
48	0.999(37)

TABLE XIII. Results of the fits of $A(N_t)$ according to Eq. (44) truncated at the order $O(x^6)$ i.e. $O(N_t^{12})$.

β	γ_3	γ_5	χ_r^2
0.751800	-0.00057(3)	0.00000038(3)	1.11
0.756427	-0.00046(3)	0.00000028(3)	1.54
0.758266	-0.00049(3)	0.00000031(3)	1.09

Looking at these results we see that there is a remarkable agreement between the values of γ_3 and γ_5 obtained with this method and those obtained in the previous section with the snake algorithm. We also see, as anticipated, that with this method there is a significant decrease of the uncertainty on the determination of γ_3 and that the values obtained (with both methods) for $\beta = 0.751800$ do not agree within the errors with those obtained with the other two values of β . This suggests that, within the precision of our analysis, $\beta = 0.751800$ is still slightly outside the scaling window, while the data for $\beta = 0.756427$ and $\beta = 0.758266$ agree between them thus showing a good scaling behavior.

We quote as our final result,

$$\gamma_3 = -0.00048(4), \quad \gamma_5 = 3.0(4) \times 10^{-7}, \quad (45)$$

obtained combining together the values obtained at $\beta = 0.756427$ and $\beta = 0.758266$ with the present approach. These values are compatible within the errors with the value obtained with the snake algorithm at $\beta = 0.756427$.

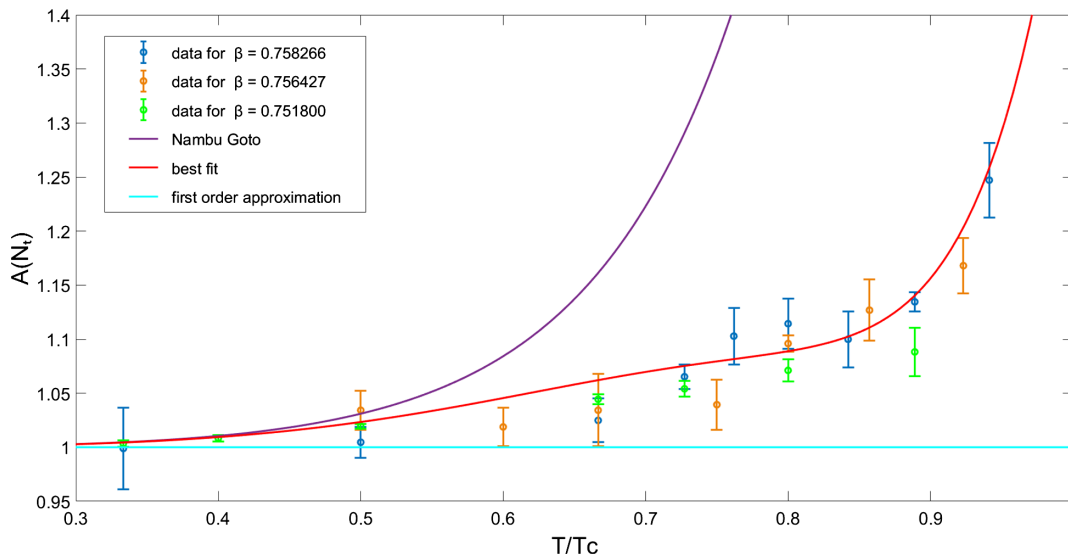


FIG. 1. Values of $A(N_t)$ for the three different values of β . The horizontal line corresponds to the first-order approximation in which the EST is truncated to the Lüscher term only, the violet curve is the Nambu-Goto prediction (truncated at the order x^6) and the red one is the prediction of Eq. (44) with the best-fit values of γ_3 and γ_5 for $\beta = 0.758266$.

VII. CONCLUDING REMARKS

We studied, using two different methods and different algorithms the correction beyond Nambu-Goto for the confining potential in the three-dimensional gauge Ising model. We found a good agreement between the two approaches. The two largest values of β that we studied show a good scaling behavior and lead to values for γ_3 and γ_5 compatible within the errors. Our final estimate for these parameters is $\gamma_3 = -0.00048(4)$ and $\gamma_5 = 3.0(4) \times 10^{-7}$.

The value that we obtained for γ_3 agrees with the bound of Eq. (22), while γ_5 is slightly below the bound of Eq. (21) which, inserting the value of γ_3 and keeping into account the uncertainty in the determination of γ_3 , becomes $\gamma_5 > 1.6 \times 10^{-6}$. This difference is most probably due to the truncation in the perturbative expansion. Keeping into account higher-order terms, and including also γ_7 might fill this gap.

It is interesting to compare our result with the existing estimates for γ_3 for other LGTs. In [27] it was shown that also for the $SU(2)$ LGT in three-dimensional γ_3 is negative. The value quoted in [27] is $\gamma_3|_{SU(2)} = -0.00037(6)$ which is similar, but not compatible within the errors, with the one we obtained here for the Ising model. On the contrary, for $SU(6)$ a positive value $\gamma_3 \approx 3 \times 10^{-4}$ was found [19,33,34]. These values represent the first steps toward a classification of EST models for LGTs. Indeed, in the past years, one of the main problems of the EST description of Yang-Mills theories was its universality, i.e. the fact that it predicted essentially the same behavior (with only a mild dependence on the number of spacetime dimensions), for models as different as the three-dimensional \mathbf{Z}_2 gauge model and the four-dimensional $SU(3)$ Yang-Mills theory. This feature is

now understood as a universality that manifests itself only at low-energy (or, equivalently, a side effect of the high accuracy of the Nambu-Goto approximation of EST), while the details related to the gauge group (and, possibly, to the confining mechanism into play) are instead encoded in the γ_i corrections, which are not expected to be universal. In particular, from the values quoted above, it seems that γ_3 for ordinary LGTs takes very small values, which seem to increase with the complexity and size of the gauge group. This should be contrasted with the case of the 3D $U(1)$ model where sizeable deviations from the Nambu-Goto prediction were observed in several quantities [49,66,67] which most likely point to a much larger, positive value of γ_3 .

Finally, let us add a comment on the numerical side of our analysis. As we have seen, duality plays a crucial role in our analysis and for this reason the approach discussed in this paper is particularly suited for Abelian gauge theories, however, apart from the numerical convenience, there is no obstruction to extend the flux based method discussed in Sec. VI, given enough computational power, also to non-Abelian models. Moreover we have seen that with this approach the error in the determination of $A(N_t)$ is dominated by the statistical uncertainty while the systematic error due to σ and α is fully negligible. This means that there would be in principle no obstruction to improve the estimates of γ_3 and γ_5 with a larger statistics.

ACKNOWLEDGMENTS

We thank F. Gliozzi, A. Guerrieri, A. Nada and M. Panero for several useful discussions and for a careful reading of the first version of the draft. We acknowledge

support from the SFT Scientific Initiative of INFN. This work was partially supported by the Simons Foundation Grant No. 994300 (Simons Collaboration on Confinement and QCD Strings) and by the Prin 2022 Grant No. 2022ZTPK4E.

APPENDIX: EVALUATION OF $\alpha(\beta)$

A first approximation for α can be obtained assuming the known scaling behavior for the string tension in the 3D gauge Ising model

$$\sigma(\beta) = \sigma_c(\beta_c - \beta)^{2\nu}$$

which leads to a simple and elegant expression for α

$$\alpha(\beta) = \frac{2\nu\sigma}{3N_s^2(\beta_c - \beta)}.$$

However this is not enough for our purposes. In order to estimate higher-order effective string corrections we need

to evaluate the flux density with an uncertainty smaller than 1% and thus it is mandatory to include in the expression the next to leading terms of the scaling function. Following [50] and using the results of [41] we can approximate the scaling function as

$$\sigma(\beta) = \sigma_c t^{2\nu} \times (1 + at^\theta + bt),$$

where $t = \tilde{\beta} - \tilde{\beta}_c$ is the dual of the reduced temperature, $\theta = 0.5241(33)$ is the next to leading scaling exponent and the constants take the following values: $\sigma_c = 10.083(8)$, $a = -0.479(26)$ and $b = -2.12(19)$.

Inserting this correction in the definition of α and approximating for simplicity $2\theta \sim 1$ we finally obtain

$$\alpha(\beta) = \frac{2\nu\sigma}{3N_s^2(\beta_c - \beta)} \left[1 + \frac{a\theta}{2\nu} t^\theta + \frac{(b - a^2)\theta}{2\nu} t \right].$$

This is the expression that we used to obtain the values listed in Table VIII.

-
- [1] Y. Nambu, Strings, monopoles and gauge fields, *Phys. Rev. D* **10**, 4262 (1974).
 - [2] T. Goto, Relativistic quantum mechanics of one-dimensional mechanical continuum and subsidiary condition of dual resonance model, *Prog. Theor. Phys.* **46**, 1560 (1971).
 - [3] M. Luscher, Symmetry breaking aspects of the roughening transition in gauge theories, *Nucl. Phys.* **B180**, 317 (1981).
 - [4] M. Luscher, K. Symanzik, and P. Weisz, Anomalies of the free loop wave equation in the WKB approximation, *Nucl. Phys.* **B173**, 365 (1980).
 - [5] J. Polchinski and A. Strominger, Effective string theory, *Phys. Rev. Lett.* **67**, 1681 (1991).
 - [6] H. B. Meyer, Poincare invariance in effective string theories, *J. High Energy Phys.* **05** (2006) 066.
 - [7] M. Luscher and P. Weisz, String excitation energies in SU(N) gauge theories beyond the free-string approximation, *J. High Energy Phys.* **07** (2004) 014.
 - [8] O. Aharony and E. Karzbrun, On the effective action of confining strings, *J. High Energy Phys.* **06** (2009) 012.
 - [9] O. Aharony and M. Dodelson, Effective string theory and nonlinear Lorentz invariance, *J. High Energy Phys.* **02** (2012) 008.
 - [10] S. Dubovsky, R. Flauger, and V. Gorbenko, Effective string theory revisited, *J. High Energy Phys.* **09** (2012) 044.
 - [11] M. Billo, M. Caselle, F. Gliozzi, M. Meineri, and R. Pellegrini, The Lorentz-invariant boundary action of the confining string and its universal contribution to the interquark potential, *J. High Energy Phys.* **05** (2012) 130.
 - [12] F. Gliozzi and M. Meineri, Lorentz completion of effective string (and p-brane) action, *J. High Energy Phys.* **08** (2012) 056.
 - [13] O. Aharony and Z. Komargodski, The effective theory of long strings, *J. High Energy Phys.* **05** (2013) 118.
 - [14] B. B. Brandt and M. Meineri, Effective string description of confining flux tubes, *Int. J. Mod. Phys. A* **31**, 1643001 (2016).
 - [15] M. Caselle, Effective string description of the confining flux tube at finite temperature, *Universe* **7**, 170 (2021).
 - [16] M. Caselle, D. Fioravanti, F. Gliozzi, and R. Tateo, Quantisation of the effective string with TBA, *J. High Energy Phys.* **07** (2013) 071.
 - [17] S. Dubovsky, R. Flauger, and V. Gorbenko, Solving the simplest theory of quantum gravity, *J. High Energy Phys.* **09** (2012) 133.
 - [18] S. Dubovsky, R. Flauger, and V. Gorbenko, Evidence from lattice data for a new particle on the worldsheet of the QCD flux tube, *Phys. Rev. Lett.* **111**, 062006 (2013).
 - [19] S. Dubovsky, R. Flauger, and V. Gorbenko, Flux tube spectra from approximate integrability at low energies, *J. Exp. Theor. Phys.* **120**, 399 (2015).
 - [20] P. Cooper, S. Dubovsky, V. Gorbenko, A. Mohsen, and S. Storace, Looking for integrability on the worldsheet of confining strings, *J. High Energy Phys.* **04** (2015) 127.
 - [21] S. Dubovsky and V. Gorbenko, Towards a theory of the QCD string, *J. High Energy Phys.* **02** (2016) 022.
 - [22] P. Conkey and S. Dubovsky, Four loop scattering in the Nambu-Goto theory, *J. High Energy Phys.* **05** (2016) 071.

- [23] S. Dubovsky, V. Gorbenko, and M. Mirbabayi, Asymptotic fragility, near AdS₂ holography and $T\bar{T}$, *J. High Energy Phys.* **09** (2017) 136.
- [24] S. Dubovsky, V. Gorbenko, and G. Hernández-Chifflet, $T\bar{T}$ partition function from topological gravity, *J. High Energy Phys.* **09** (2018) 158.
- [25] J. Elias Miró, A. L. Guerrieri, A. Hebbar, J. a. Penedones, and P. Vieira, Flux tube S-matrix bootstrap, *Phys. Rev. Lett.* **123**, 221602 (2019).
- [26] J. Elias Miró and A. Guerrieri, Dual EFT bootstrap: QCD flux tubes, *J. High Energy Phys.* **10** (2021) 126.
- [27] F. Caristo, M. Caselle, N. Magnoli, A. Nada, M. Panero, and A. Smecca, Fine corrections in the effective string describing SU(2) Yang-Mills theory in three dimensions, *J. High Energy Phys.* **03** (2022) 115.
- [28] M. Billo and M. Caselle, Polyakov loop correlators from D0-brane interactions in bosonic string theory, *J. High Energy Phys.* **07** (2005) 038.
- [29] M. Billo, M. Caselle, and R. Pellegrini, New numerical results and novel effective string predictions for Wilson loops, *J. High Energy Phys.* **01** (2012) 104.
- [30] M. Billo, M. Caselle, and L. Ferro, The partition function of interfaces from the Nambu-Goto effective string theory, *J. High Energy Phys.* **02** (2006) 070.
- [31] P. Olesen, Strings, tachyons and deconfinement, *Phys. Lett.* **160B**, 408 (1985).
- [32] R. D. Pisarski and O. Alvarez, Strings at finite temperature and deconfinement, *Phys. Rev. D* **26**, 3735 (1982).
- [33] A. Athenodorou, B. Bringoltz, and M. Teper, Closed flux tubes and their string description in $D = 2 + 1$ SU(N) gauge theories, *J. High Energy Phys.* **05** (2011) 042.
- [34] C. Chen, P. Conkey, S. Dubovsky, and G. Hernández-Chifflet, Undressing confining flux tubes with $T\bar{T}$, *Phys. Rev. D* **98**, 114024 (2018).
- [35] A. Athenodorou and M. Teper, Closed flux tubes in $D = 2 + 1$ SU(N) gauge theories: Dynamics and effective string description, *J. High Energy Phys.* **10** (2016) 093.
- [36] O. Aharony and M. Field, On the effective theory of long open strings, *J. High Energy Phys.* **01** (2011) 065.
- [37] B. B. Brandt, Probing boundary-corrections to Nambu-Goto open string energy levels in 3d SU(2) gauge theory, *J. High Energy Phys.* **02** (2011) 040.
- [38] B. B. Brandt, Spectrum of the open QCD flux tube and its effective string description I: 3d static potential in SU(N = 2, 3), *J. High Energy Phys.* **07** (2017) 008.
- [39] B. B. Brandt, Revisiting the flux tube spectrum of 3d SU(2) lattice gauge theory, *Indian J. Phys.* **95**, 1613 (2021).
- [40] M. Caselle, R. Fiore, F. Gliozzi, M. Hasenbusch, K. Pinn, and S. Vinti, Rough interfaces beyond the Gaussian approximation, *Nucl. Phys.* **B432**, 590 (1994).
- [41] M. Caselle, M. Hasenbusch, and M. Panero, The interface free energy: Comparison of accurate Monte Carlo results for the 3D Ising model with effective interface models, *J. High Energy Phys.* **09** (2007) 117.
- [42] M. Caselle, G. Costagliola, A. Nada, M. Panero, and A. Toniato, Jarzynski's theorem for lattice gauge theory, *Phys. Rev. D* **94**, 034503 (2016).
- [43] M. Caselle, A. Feo, M. Panero, and R. Pellegrini, Universal signatures of the effective string in finite temperature lattice gauge theories, *J. High Energy Phys.* **04** (2011) 020.
- [44] M. Caselle, R. Fiore, F. Gliozzi, M. Hasenbusch, and P. Provero, String effects in the Wilson loop: A high precision numerical test, *Nucl. Phys.* **B486**, 245 (1997).
- [45] P. de Forcrand, M. D'Elia, and M. Pepe, A Study of the 't Hooft loop in SU(2) Yang-Mills theory, *Phys. Rev. Lett.* **86**, 1438 (2001).
- [46] M. Caselle, M. Hasenbusch, and M. Panero, String effects in the 3-d gauge Ising model, *J. High Energy Phys.* **01** (2003) 057.
- [47] M. Caselle, M. Hasenbusch, and M. Panero, Short distance behaviour of the effective string, *J. High Energy Phys.* **05** (2004) 032.
- [48] M. Caselle, M. Hasenbusch, and M. Panero, Comparing the Nambu-Goto string with LGT results, *J. High Energy Phys.* **03** (2005) 026.
- [49] M. Caselle, M. Panero, R. Pellegrini, and D. Vadicchino, A different kind of string, *J. High Energy Phys.* **01** (2015) 105.
- [50] M. Caselle and M. Zago, A new approach to the study of effective string corrections in LGTs, *Eur. Phys. J. C* **71**, 1658 (2011).
- [51] F. J. Wegner, Duality in generalized Ising models and phase transitions without local order parameters, *J. Math. Phys.* (N.Y.) **12**, 2259 (1971).
- [52] A. Athenodorou, S. Dubovsky, C. Luo, and M. Teper, Excitations of Ising strings on a lattice, *J. High Energy Phys.* **05** (2023) 082.
- [53] M. Caselle, M. Hasenbusch, and M. Panero, On the effective string spectrum of the tridimensional Z(2) gauge model, *J. High Energy Phys.* **01** (2006) 076.
- [54] V. Agostini, G. Carlino, M. Caselle, and M. Hasenbusch, The spectrum of the (2 + 1)-dimensional gauge Ising model, *Nucl. Phys.* **B484**, 331 (1997).
- [55] M. Hasenbusch, Thermodynamic casimir effect: Universality and corrections to scaling, *Phys. Rev. B* **85**, 174421 (2012).
- [56] M. Hasenbusch and K. Pinn, Computing the roughening transition of Ising and solid-on-solid models by BCSOS model matching, *J. Phys. A* **30**, 63 (1997).
- [57] M. Caselle and M. Hasenbusch, Deconfinement transition and dimensional crossover in the 3-D gauge Ising model, *Nucl. Phys.* **B470**, 435 (1996).
- [58] R. Savit, Duality in field theory and statistical systems, *Rev. Mod. Phys.* **52**, 453 (1980).
- [59] F. Kos, D. Poland, D. Simmons-Duffin, and A. Vichi, Precision Islands in the Ising and $O(N)$ models, *J. High Energy Phys.* **08** (2016) 036.
- [60] D. Poland, S. Rychkov, and A. Vichi, The conformal bootstrap: Theory, numerical techniques, and applications, *Rev. Mod. Phys.* **91**, 015002 (2019).
- [61] M. Caselle, M. Hasenbusch, P. Provero, and K. Zarembo, Bound states and glueballs in three-dimensional Ising systems, *Nucl. Phys.* **B623**, 474 (2002).
- [62] F. Gliozzi, M. Pepe, and U. J. Wiese, The width of the confining string in Yang-Mills theory, *Phys. Rev. Lett.* **104**, 232001 (2010).

- [63] A. Allais and M. Caselle, On the linear increase of the flux tube thickness near the deconfinement transition, *J. High Energy Phys.* 01 (2009) 073.
- [64] M. Caselle, Flux tube delocalization at the deconfinement point, *J. High Energy Phys.* 08 (2010) 063.
- [65] M. Caselle, F. Gliozzi, U. Magnea, and S. Vinti, Width of long color flux tubes in lattice gauge systems, *Nucl. Phys.* **B460**, 397 (1996).
- [66] M. Caselle, M. Panero, and D. Vadicchino, Width of the flux tube in compact U(1) gauge theory in three dimensions, *J. High Energy Phys.* 02 (2016) 180.
- [67] M. Caselle, A. Nada, M. Panero, and D. Vadicchino, Conformal field theory and the hot phase of three-dimensional U(1) gauge theory, *J. High Energy Phys.* 05 (2019) 068.